HFCT-based Detection of Partial Discharge Currents on GIS Enclosures

L. C. Castro Heredia and A. Rodrigo Mor
Department of Electrical Sustainable Energy
Delft University of Technology
Delft, The Netherlands

***Abstract*- This work introduces an approach for partial discharge (PD) detection on GIS that makes use of HFCT. The novelty of this method is that the HFCT is installed at the bolts of the external-type spacers to measure, with a bandwidth in the range of hundreds of MHz, the induced PD surface currents flowing along the GIS compartments. Experiments with calibrator signals were conducted to prove that the PD events induce currents in the compartments and to understand their distribution. Next, measurements with test cells were carried out to estimate the spatial sensitivity of the measuring circuit and the effect of noise and disturbances. Finally, the spectral power ratio clustering technique was applied to test results as a method to discriminate PD and non-PD signals.**

I. INTRODUCTION

Gas insulated systems (GIS) are components of the HV networks especially suitable when the overall size of a substation needs to be scaled down. This becomes cornerstone in offshore applications where the price and availability of space comes to a high premium. For a reliable operation, GIS are equipped with VHF/UHF antennas for the monitoring and diagnostics of partial discharges (PD). Documents such as the IEC TS 62478 [1] and CIGRE WG. D1.25 [2] offer good reference guidelines for implementation and also define a "sensitivity check" as a means to verify that a VHF/UHF measuring system on-field is able to pick up signals equivalent to 5 pC as measured by the conventional IEC 60270 method during laboratory tests. Several decades of field experience have supported that the VHF/UHF systems are sensitive and high resilient to noise due to the high frequency range at which they record PD signals. Nevertheless, this high frequency range also accounts for some important limitations according to the IEC TS 62478. A correlation of the measured signal to an apparent charge is not possible because the resonating frequency of the antenna in the range of hundreds of MHz to GHz is far away from the DC component (or low frequency components) of the PD current that needs to be measured to estimate the value of apparent charge. In addition, the GHz range of the UHF systems demands acquisition units with higher requirements. The antennas, having a GIS-dependent design, also contributes to step up the overall cost of this type of system. Moreover, its complexity may soar due to the number of antennas that are required to monitor a long GIS.

While it is true that going up in frequency is desirable to reduce the effect of noise and disturbances, lowering the measuring frequency range may downplay the requirements of a VHF/UHF system and increase its spatial sensitivity. Thus, the aim of this paper is to present experimental results of an alternative approach for measuring PD in the low frequency range. In the following sections, it will be documented how this approach uses HFCT sensors installed conveniently at the GIS spacers to measure the induced currents on the GIS compartments by a PD event. In addition, it will be demonstrated by laboratory measurements that in such a low frequency range the attenuation of the PD-induced currents is lower which may be seized to enhance the spatial sensitivity. Finally, the limitations and the effect of noise and disturbances in this frequency range will be commented.

II. TEST OBJECT

All the laboratory measurements here reported were conducted on the actual size, 380kV GIS of Figure 1, comprised of spacers, T-joints, a bushing, a disconnector switch, a ground switch and a circuit breaker.

The GIS end at the bottom of the Figure 1 was utilized to place test cells to produce corona and surface discharges and to connect a pulse calibrator. The arrangement of sensors consisted of an HFCT at the GIS end labeled as "source HFCT" and two HFCT installed at the spacers in position 1 and 2 ("HFCT 1" and "HFCT 2"). A Tektronix MSO5 oscilloscope recorded simultaneously the signals from every sensor. Test voltages, SF6 pressure and amplifier specifications for each test are summarized in Table 1. It is important to mention that all the voltage signals reported in the following sections correspond to the voltage at the output of the amplifiers, not the voltage at the HFCT output.

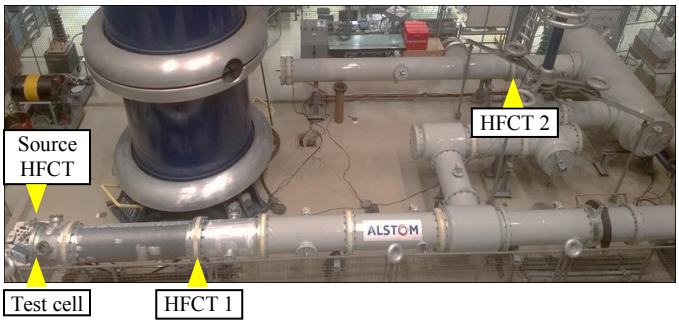

Fig. 1. Test object and location of HFCT sensors.

978-1-5386-8434-4/19/$31.00 ©2019 IEEE

TABLE I. Test Parameters.

	Corona	Surface
Source HFCT	Sensor: 5 mV/mA, BW 3.92 kHz-1.11 GHz Amp: 26dB, BW 100 kHz-1.3 GHz	
HFCT 1	Sensor: 9.1 mV/mA, BW 62 kHz-136 MHz Amps: 50.4dB, 30 kHz-1.23 GHz	
HFCT 2	Sensor: 9.1mV/mA, BW 62 kHz-136 MHz Amps: 44.4dB, 30 kHz-1.23 GHz	
V_{AC}	15 kV_{RMS}	20 kV_{RMS}
SF_6	3 Bar	1.2 Bar

III. PD-INDUCED CURRENTS IN THE GIS COMPARTMENTS

The main concept that plays a role for the detection of PD pulses in GIS is that upon a fast PD event, electromagnetic waves are excited which travel guided by the transmission line structure of the GIS. The way the propagation of the PD signal occurs depends on the frequency range of the PD spectrum. At sufficiently high frequencies, the transverse electric (TE) and transverse magnetic (TM) are the predominant propagation modes of PD electromagnetic waves and each of these modes has a cut-off frequency below which it will not propagate [3][4][5]. UHF antennas resonates at these frequencies picking up the radio frequency energy of the PD pulse. At lower frequencies, the propagation follows the transverse electromagnetic (TEM) mode which suffers from less attenuation than the other high frequency modes. This is the phenomena seized in our approach with the particularity that an HFCT is used to measure the induced PD currents in the GIS compartments instead of UHF antennas to measure radiated energy.

The measuring arrangement to do so consists of an HFCT installed at one of the bolts of a spacer as depicted in Figure 2. Note that at the spacer location, the PD current pulse flows along the bolts before reaching the next compartment. Insulating sleeves in the bolts make the current to flow first through the sensor before returning to the compartment and therefore the HFCT is enabled to measure the PD signal flowing in the compartments.

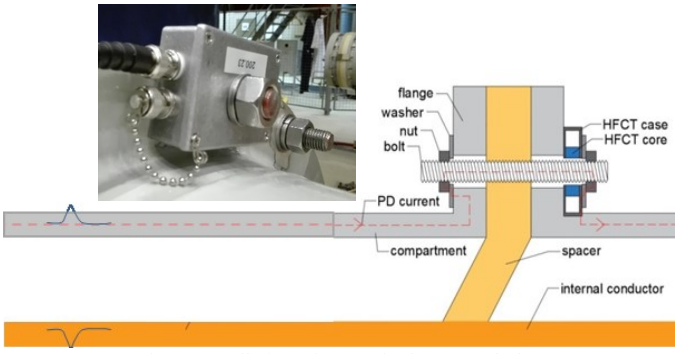

Fig. 2. Installation of HFCT in the spacer bolts.

The GIS used in this work has 16 bolts connecting two adjacent compartments, therefore a part of the PD current should flow along each of these bolts. Likewise, other questions arise from this measuring approach such as: is the current evenly distributed among all the bolts?, how do the noise and disturbances affect the sensitivity?, is the spatial sensitivity better than that of the UHF systems?

In the following subsection a set of experiments were conducted to answer these questions.

A. *Current Distribution and Attenuation*

To determine the current distribution and attenuation a calibrator signal was injected at the GIS end and the signals from the source HFCT and HFCTs at location 1 were recorded.

Three configurations were used. Measurements in configuration 1 consisted of having only one sensor installed at the spacer while the remaining 15 bolts were unchanged. In configuration 2, four sensors were installed, and the remaining 12 bolts were unchanged. In configuration 3, only one sensor was installed but the remaining 15 bolts were insulated so the current only flowed along the bolt having the sensor installed.

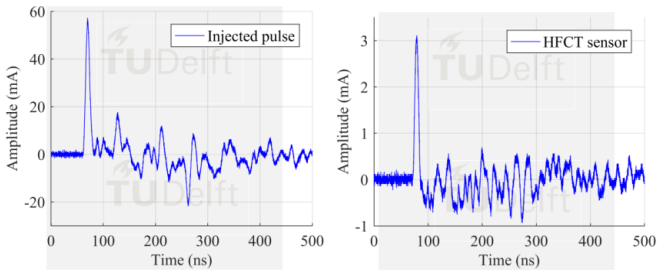

Fig. 3. Results from configuration 1.

Results from configuration 1 in Figure 3 indicated that the peak amplitude of the HFCT 1 signal was 5.43% that of the source HFCT. This ratio is quite close to the 6.25% that is expected if the current is split equally into the 16 bolts, the difference possibly coming as a result of the transfer impedance of the HFCT added to the path. Moreover, this results already suggests that the current flows evenly distributed along the compartment. In order to further prove this claim, measurements in configuration 2 were carried out and its results displayed in Figure 4.

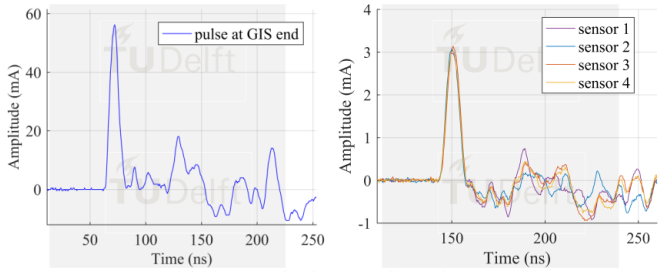

Fig. 4. Results from configuration 2.

The amplitude of the four sensors was nearly equal to that of the sensor in configuration 1, yielding a ratio of 5.51% confirming that the current along each bolt can be considered the same.

Configuration 3 came as an attempt to increase the sensitivity of the sensor by forcing all of the current through the sensor. However, as shown in Figure 5, there was a mismatch of the amplitude of the injected pulse and that of the HFCT 1. The shape of the HFCT 1 pulse also showed a big undershoot, which led to the conclusion that in this configuration the transmission line structure of the GIS is broken and the effect of reflections of the pulse is significant as to lead to major errors in the quantification of the signal amplitude. In consequence, configuration 1 was preferred for the experiments with PD test cells.

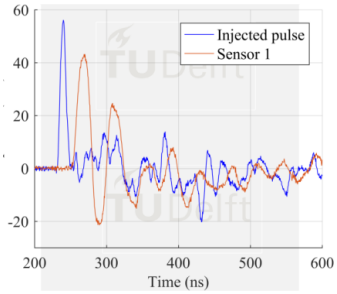

Fig. 5. Results from configuration 3.

IV. Measurements with Test Cells

Experiments with the test cells had the purpose of verifying that the signals from the HFCT at location 1 and 2 correspond to actual PD signals and checking the attenuation of the signals with distance.

The first step in this verification procedure was to collect the PRPD patterns (Figure 6) produced by the test cells (measured with the HFCT at the source) that will be used as the reference PD signals.

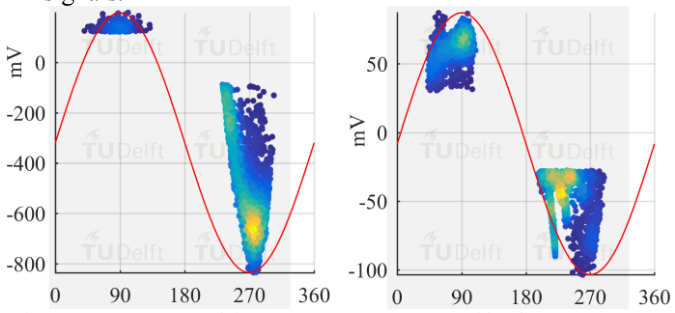

Fig. 6. PRPD patterns of the two PD sources measured by the source HFCT.

Because the source HFCT was used as the trigger of the oscilloscope, then the phase of the PRPD patterns obtained from HFCT 1 and 2 necessarily was the same as that of patterns in Figure 6. The amplitude and pulse shape, however, needed to be screened in order to verify that the recorded signals corresponded to the actual PD pulses that triggered the acquisition.

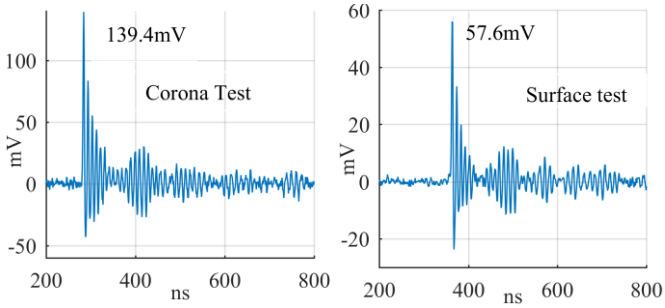

Fig. 7. Smallest PD signals recorded by the source HFCT.

By using the software *PDflex* [6] the signals from all the sensors were contrasted resulting in that the test-cell PD pulses with the highest amplitude were recorded properly by the HFCT 1 and 2. With decreased amplitude disturbances and noise were easier to be coupled to the sensors. For instance, consider signals in Figure 7 corresponding to one of the smallest signals of the PRDP patterns in Figure 6. As shown in Figure 8 and 9 (signals corresponding to the signals in Figure 7), the SNR decreased and signals from HFCT 2 are notably affected by reflections produced as the PD pulse travels along the GIS components.

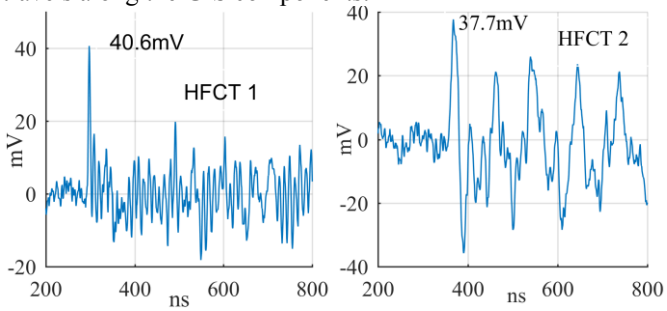

Fig. 8. Smallest corona signals recorded by HFCT 1 and 2.

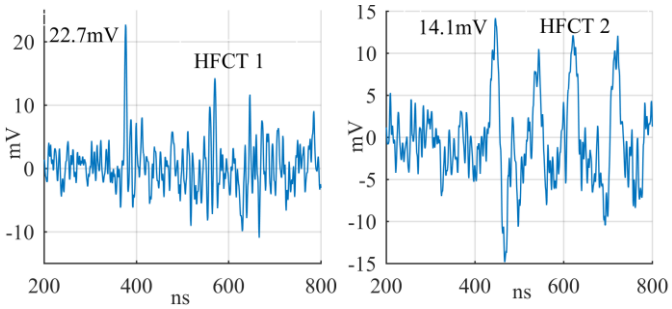

Fig. 9. Smallest surface signals recorded by HFCT 1 and 2.

Nevertheless, these results also prove that the sensitivity of the HFCT at the spacers may be enough to pick up PD signals produced at the test cell 16 m away. A contribution from the authors in [7] reported that an UHF antenna installed next to HFCT 1 picked up also a true PD signal but didn't do so when located next to HFCT 2.

In a real implementation, the trigger source certainly would have to be one HFCT installed at a given spacer in which case a low SNR, disturbances and noise may imply false acquisitions, i.e. recording of signals not corresponding to PD pulses. It is a matter of fact that this is one of the limitations of the HFCT-based PD detection reported in this work, although it does not necessarily mean that acquisition and clustering

techniques cannot be applied as a possible mitigation of this limitation. This is tested in the next section.

V. HFCT-BASED DETECTION IN PRESENCE OF NOISE

For these measurements, the surface test cell was utilized, the oscilloscope was set to acquire 5000 frames and the signal from the HFCT 1 was the trigger source. At the moment of the measurements, other experiments were running in the laboratory that created a big deal of disturbances and noise leading to the blurred PRPD pattern of Figure 10. Exemplary waveforms from different locations of the pattern are also displayed to contrast the difference between PD (Figure 10b) and non-PD signals (Figure 10c and d).

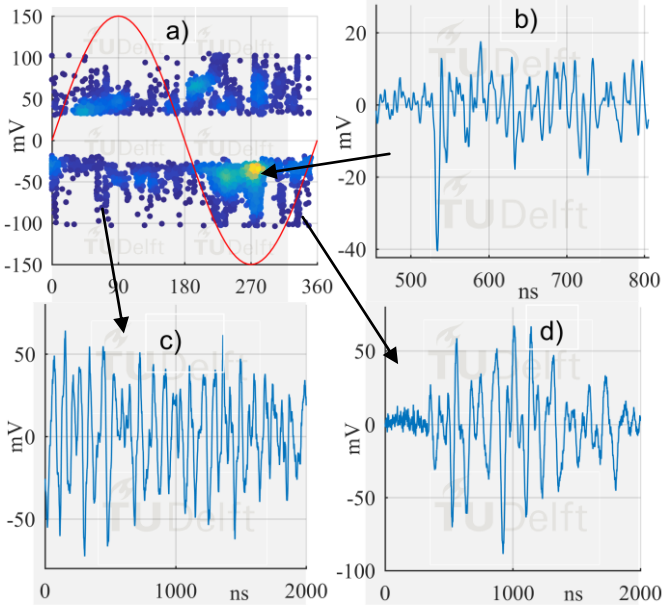

Fig. 10. a) Surface PRPD pattern from HFCT 1, b) PD pulse, c) disturbance, d) disturbance.

Subsequently, the power ratio clustering technique [8] was applied to the data. After the screening of the data in red in Figure 11a, it was confirmed that the clustering technique managed to extract the PD pulses from the noise and disturbances. 1113 out of 5000 were clustered as actual PD signals. The PRPD pattern in Figure 11b constructed with the clustered data now can be recognized as a surface pattern and matches fairly good the one in Figure 6.

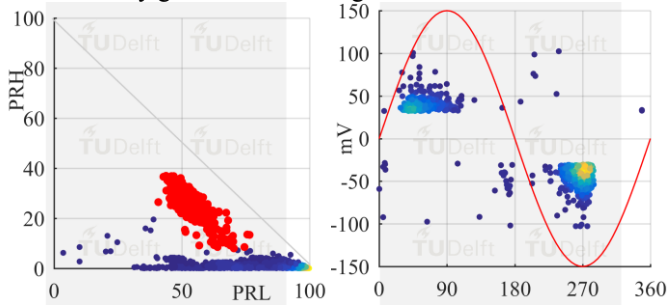

Fig. 11. a) Spectral power cluster, b) Surface PRPD pattern after clustering.

VI. CONCLUSION

In this paper, an approach to detect partial discharges in GIS by HFCT installed at the bolts of the spacers has been introduced. By laboratory measurements, it was proven that the PD event induces currents in the compartments which in practice can be picked up by an HFCT because the currents flowing along the compartments split homogenously among the bolts connecting two adjacent compartments. Advantages of this approach are an increased spatial sensitivity, lower requirements for the acquisition unit as the bandwidth is reduced down to hundreds of MHz, and potential for charge estimation since the measured signal might be correlated to the actual PD signal at its source. However, this will require further research not covered by this paper. Disadvantages also arise such as the vulnerability of the system to disturbances and noise in the frequency range of the HFCT, the effect of reflections on the measured signal that jeopardize the quantification and extraction of parameters from the pulse shape and that the installation of the HFCT as described here only is feasible with GIS designs having "external" spacers.

ACKNOWLEDGMENT

This project has received funding from the European Union's Horizon 2020 research and innovation programme under grant agreement No. 691714.

REFERENCES

[1] IEC-TS-62478, High voltage test techniques – Measurement of partial discharges by electromagnetic and acoustic methods, 2016

[2] CIGRE WG. D1.25, UHF partial discharge detection system for GIS: Application guide for sensitivity verification, 2016.

[3] K. Mizuno et al., Investigation of PD pulse propagation characteristics in GIS. In Proceedings of Transmission and Distribution Conference and Exposition, Los Angeles, CA, USA, 1996..

[4] H. Muto, M. Doi, H. Fujii, and M. Kamei, Resonance characteristics and identification of modes wave excited by partial discharges in GIS. In Eleventh International Symposium on High Voltage Engineering, London, UK, 1999

[5] CIGRE TF. 15/33.03.05, Partial discharge detection system for GIS: sensitivity verification for the UHF method and the acoustic method, 1999.

[6] PDflex – Unconventional Partial Discharge Analysis. Available at: http://pdflex.tudelft.nl (accessed 6 December 2018).

[7] A. Rodrigo Mor, L. C. Castro-Heredia, and F. A. Muñoz, "A Novel Approach for partial discharge measurements on GIS using HFCT sensors," accepted for publication in *Sensors*, 2018.

[8] J. Ardila-Rey, J. Martínez-Tarifa, G. Robles, and M. Rojas-Moreno, "Partial discharge and noise separation by means of spectral-power clustering techniques," *IEEE Trans. Dielectr. Electr. Insul.*, vol. 20, no. 4, pp. 1436–1443, Aug. 2013.